Available online at www.sciencedirect.com

ScienceDirect

Applied Mathematical Modelling 31 (2007) 1798–1806

APPLIED MATHEMATICAL MODELLING

www.elsevier.com/locate/apm

Analysis of filling distance in cylindrical microfeatures for microinjection molding

Wen-Bin Young *

National Cheng-Kung University, Institute of Aeronautics and Astronautics, Tainan 70101, Taiwan, ROC

Received 1 June 2005; received in revised form 1 May 2006; accepted 12 June 2006
Available online 1 August 2006

Abstract

In the injection molding of plastic components with cylindrical microfeatures, the ability for the polymer melt to flow into the microchannels is a crucial factor for successful molding. Penetration distance of the polymer melt into the microstructure depends on several factors as the melt flow rate and the cooling rate in the microfeatures, which depends on the materials and geometric dimensions. In this study, a simplified analytical model was constructed to estimate the filling distance into the cylindrical microchannels. The effects of the mold temperature, injection rate, heat transfer coefficient, and microchannel dimension on the filling distance were investigated. The filling distance decreases dramatically with respect to the decrease of the channel radius. In molding of plastic components with cylindrical microfeatures as those analyzed in this study, decrease of the part thickness could also increase the filling distance in the microfeatures.

Keywords: Microinjection molding; LIGA-like process; Micromolding; Molding simulation

1. Introduction

Microinjection molding is one of the methods to fabricate microscale plastic components. It is an injection molding process, but generally designated to the fabrication of components with microfeatures or components with volumes in the range of milligrams. Potential applications of these components include plastic optics, microfluidics, biochips, micromechanical components, micro-Total Analysis Systems, etc. The application in the plastic optics and biochips requires fabricating a plastic substrate with microfeatures on it. The process of molding a component with microfeatures involves the development of mold insert with LIGA or LIGA-like processes. The LIGA process has the procedures as X-ray lithography, galvanoformung (electroforming), and abformung (molding) [1,2]. For the LIGA-like process, employment of thick layer photoresist with standard UV lithography procedures is used to fabricate the mold insert with microfeatures [3,4].

In micromolding of plastic components with microfeatures, the ability for the polymer melt to flow into the microchannels is a crucial factor for successful molding. The molded volume is about the same as the

* Tel.: +886 6 275 7575x63672; fax: +886 6 238 9940.
E-mail address: youngwb@mail.ncku.edu.tw

0307-904X/$ - see front matter
doi:10.1016/j.apm.2006.06.003

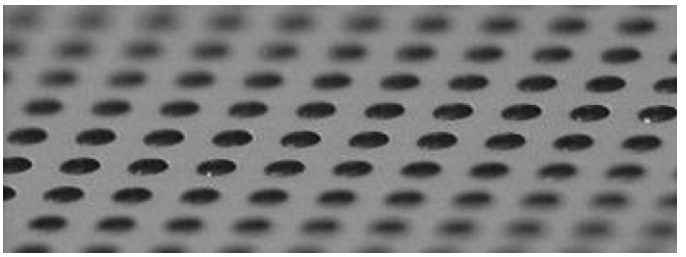

Fig. 1. A mold insert with cylindrical microfeatures.

conventional molding. Penetration distance of the polymer melt into the microstructure depends on the flow rate and the cooling rate of the microfeatures, which is function of the materials and geometric dimension. In the range of 10–100 μm features, the cooling rate of the polymer melt is so quick that the flow distance is limited to a very short distance for a mold under the room temperature. It was reported that mold temperature and injection rate were the major factors related to the micromolding [5,6]. In order to design proper microfeatures and process conditions, the processing simulation tool can be used simulate the injection process. A three-dimensional simulation must be employed in order to catch the microfeatures together with the main component. This will involve huge number of elements in the calculation. In this study, a simplified analytical model was constructed to estimate the injection distance into the cylindrical microchannels of a mold insert as shown in Fig. 1. The effect of the mold temperature, injection rate, and microchannel radius on the filling distance was investigated based on the model.

2. Microfilling model

It was reported that the flow in the microscale was different from those in the macroscale [7,8]. Viscosity was found to increase as the channel size decreased below tens of micrometers. The polymer melt was also found to slip over the wall surface as the channel size was down below about a micrometer. In this study, the channel size is limited to the range above ten micrometers so that the viscosity is not considered to depend on the channel size and the wall slip effect is also neglected. In modeling the injection flow of a component with microfeatures, the mold insert temperature is assumed to be uniform and does not vary during injection. Since the microfeature considered usually has an aspect ratio around 1–2, the fountain flow effect in the Hele–Shaw flow may not be dominant. It is assumed that the filling of the microchannel starts with the melt temperature as the initial value. During the filling, the melt cools down due to the heat flow through the mold wall. A constant heat transfer coefficient is also assumed in the interface of the melt and mold wall. The melt at the interface is close to the mold temperature for a high value of heat transfer coefficient. On the other hand, it is close to adiabatic for a low value. A power law fluid model is assumed for the polymer melt. In calculation of the viscosity, an average temperature across the channel is used. The filling flow will stop as the temperature drops below the transition temperature. The assumptions are made to simply the model in order to derive a close form solution for understand the effect of the processing parameters on the filling ability of the microfeature.

During the injection, polymer melt will fill the main cavity and the microfeatures at the same time. If a single channel is considered, the local filling of the flow front near the microchannel is shown in Fig. 2. The injection rate, Q, is considered to be constant during the injection stage. If the volume in the microfeature is far small as compared to the main cavity, the amount of melt flow rate in the main cavity can be assumed to be the same as the injection rate. For one-dimensional viscous flow, the momentum equation can be expressed as

$$\frac{\mathrm{d}P}{\mathrm{d}x} = \frac{\mathrm{d}}{\mathrm{d}y}\left(\mu \frac{\mathrm{d}u}{\mathrm{d}y}\right), \tag{1}$$

where μ is the viscosity and, for a power law fluid, can be written as

$$\mu = m_x \dot{\gamma}^{n-1}, \tag{2}$$

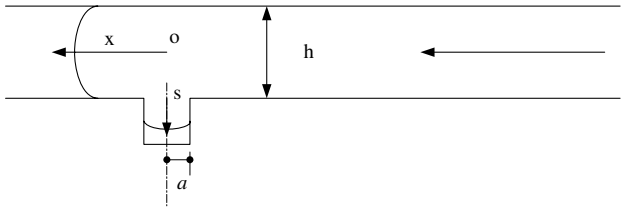

Fig. 2. Filling of the macrochannel and microchannel.

where $\dot{\gamma}$ is the shear rate and n is the power law index. If the injection time is short and the thickness of the main cavity, h, is large enough so that the temperature during the injection is assumed to be about the same, m_x can be expressed as

$$m_x = m_o e^{-a_o(T_m - T_o)}, \tag{3}$$

where T_m is the melting temperature at the main cavity, and the others are material constants. Substituting Eqs. (2) and (3) into (1), one can integrate to have the velocity as

$$u = \left(\frac{1}{m_x}\right)^{\frac{1}{n}} \left(\frac{n}{n+1}\right) \left|\frac{dP}{dx}\right|^{\frac{1}{n}} \left[\left(\frac{h}{2}\right)^{\frac{n+1}{n}} - y^{\frac{n+1}{n}}\right]. \tag{4}$$

The corresponding injection flow rate can be derived by integrating across the cross section.

$$Q = \left(\frac{1}{m_x}\right)^{\frac{1}{n}} \left(\frac{2nw}{2n+1}\right) \left|\frac{dP}{dx}\right|^{\frac{1}{n}} \left(\frac{h}{2}\right)^{\frac{2n+1}{n}}, \tag{5}$$

where w is the channel width. The pressure at point o (in Fig. 2) depends on the filled distance, x_o, from the point to the flow front and can be assumed to be constant across the thickness of the main cavity, which can be expressed as following form:

$$P_o = \frac{2^{n+1}(2n+1)^n}{n^n} \frac{m_x x_o}{w^n h^{2n+1}} Q^n, \tag{6}$$

where P_o is the pressure at point o and x_o is the distance from the flow front to the point o. Since the filling rate is constant, the melt velocity at the main cavity can be written as

$$v_x = \frac{dx}{dt} = \frac{Q_x}{wh} \approx \frac{Q}{wh}. \tag{7}$$

By assuming the amount of melt flows into the microchannel is quite small, the flow rate at the main cavity, Q_x, is about the same as the injection flow rate, Q. Integrating Eq. (7) from point o to the flow front, one can have $x_o = Qt/wh$, where t is the time after the flow front flowing over the point o.

Up to this point, we analyze the flow in the main cavity by ignoring the effect of the microchannel. However, as the flow moves to the point o, polymer melt will fill both the main cavity and the microchannel at the same time. The filling of the cylindrical microchannel can be considered as a filling process with a specified pressure at the point o, P_o. The momentum equation in the microchannel can be written as

$$\frac{dP}{ds} = \frac{1}{r}\frac{d}{dr}\left(\mu r \frac{du_s}{dr}\right) \tag{8}$$

and

$$\mu = m_s \dot{\gamma}^{n-1}, \tag{9}$$

$$m_s = m_o e^{-a_o(T_s - T_o)}, \tag{10}$$

where r is along the radial direction, s is along the channel direction, u_s is the velocity along the microchannel, and T_s is the mean temperature in the channel. The pressure at the flow front can be considered to be zero.

Substituting Eqs. (9) and (10) into (8) and integrating with respect to r, the mean velocity at the cylindrical microchannel can be written as

$$v_s = \frac{ds}{dt} = \frac{2}{a^2}\left(\frac{P_o}{\beta}\right)^{\frac{1}{n}} = \frac{2^{\frac{2n+1}{n}}(2n+1)}{na^2}\left(\frac{Q}{wh^2}\right)^{\frac{n+1}{n}}\left(\frac{m_x t}{\beta}\right)^{\frac{1}{n}} \tag{11}$$

and

$$\beta = \frac{2^{n+1}(3n+1)^n}{n^n a^{3n+1}}\int_0^{s_o} m_s\, ds, \tag{12}$$

where α is the thermal diffusivity, a is the radius of the cylindrical microchannel, s_o is the filling length, and T_s is the mean temperature in the microchannel. At the instant of time, t^i, for discrete time domain, the filling distance at the microchannel can be expressed as

$$s_o^i = s_o^{i-1} + \Delta s_o^{i-1}, \tag{13}$$

$$\Delta s_o^{i-1} = \left(\frac{ds}{dt}\right)^{i-1}\Delta t^{i-1} \tag{14}$$

and

$$t^i = t^{i-1} + \Delta t^{i-1}, \tag{15}$$

$$\left(\frac{ds}{dt}\right)^{i-1} = \frac{2^{\frac{2n+1}{n}}(2n+1)}{na^2}\left(\frac{Q}{wh^2}\right)^{\frac{n+1}{n}}\left(\frac{m_x t^{i-1}}{\beta^{i-1}}\right)^{\frac{1}{n}}. \tag{16}$$

In the above analysis, temperature is not considered to vary in the main cavity during the injection. For the microchannel, cooling of the polymer melt could be tremendous due to the small radius of the channel. Heat conduction across the channel and convection along the channel were considered. A quasi-steady state was assumed at each of the time step. At the entrance of the microchannel, the temperature is set as the melt temperature, T_m. The mold wall is kept at a constant temperature T_w. The heat transfer equation in the microchannel can thus be written as

$$v_s\frac{\partial T}{\partial s} = \frac{\alpha}{r}\frac{\partial}{\partial r}\left(r\frac{\partial T}{\partial r}\right), \tag{17}$$

where r is in the radius direction of the microchannel. The associated boundary conditions are

$$T(r,0) = T_m, \tag{18}$$

$$-k\frac{\partial T(a,s)}{\partial r} = h_t[T(a,s) - T_w], \tag{19}$$

where h_t is the heat transfer coefficient and k is the thermal conductivity of the polymer. The resulting mean temperature in the microchannel is [9]

$$\frac{T_s - T_w}{T_m - T_w} = \sum_{n=1}^{\infty}\frac{4}{\lambda_n^2 a^2\left(1 + \frac{k^2}{h_t^2}\lambda_n^2\right)}e^{-\frac{\lambda_n^2 \alpha s}{v_s}} \tag{20}$$

and λ_n satisfies the following equation:

$$\frac{\lambda_n k}{h_t}J_1(\lambda_n a) = J_0(\lambda_n a), \tag{21}$$

where J_1 and J_0 are the Bessel functions. It must be noticed that the mean temperature in the microchannel is a function of s. That is the mean temperature will change along the channel. Eq. (21) also depends on the variable, v_s (the mean flow velocity in the microchannel), while the velocity itself is a function of the mean temperature through the variable β. In the calculation of the velocity at each time step, an assumed velocity was used first to determine the temperature distribution along the microchannel. The integral in Eq. (12) can thus

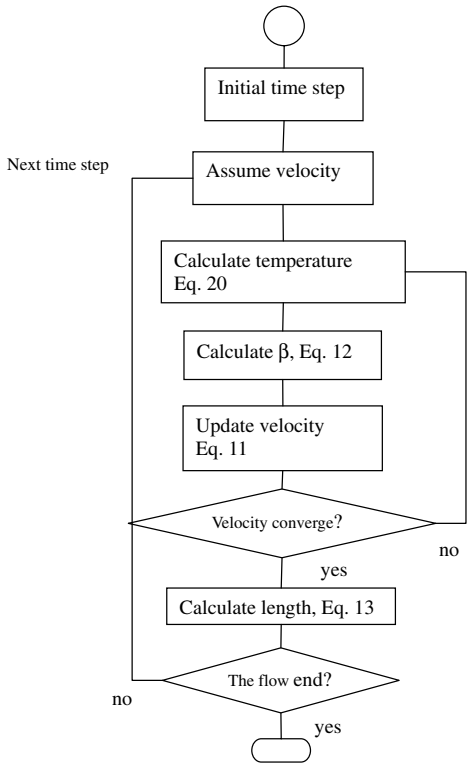

Fig. 3. The solution flowchart.

be evaluated to calculate the value of β. Then, the updating velocity can be determined by Eq. (11). Iterations are necessary until the value of velocity converges. Fig. 3 shows the list of the solution flowchart.

3. Results and discussion

In applying the current model to estimate the injection length in a cylindrical microchannel, the radius of the microchannel is set at the range of 10–100 μm. The height of the main cavity, h, is 1.2 mm and width, w, is 50 mm. The range of injection rate used is from 20 to 80 cm^3/s. The mold wall temperatures used are 20, 60, or 90 °C. Temperature of the polymer melt is set to 230 °C and the corresponding viscosity constants are listed in Table 1. The thermal diffusivity, α, is approximately 7.6×10^{-8} cm^2/s.

The velocities in the microchannel with respect to time are shown in Fig. 4 for different injection rates. The mold temperature is 90 °C. The initial value of filling velocity in the microchannel is about proportional to the injection rate. As the flow length increases, viscosity increases due to cooling the polymer melt, leading to the reduction of the velocity. As the polymer melt temperature approaching the transition temperature,

Table 1
Constants for the viscosity model

		Unit
m_o	1.234×10^6	$N\,s^n/m^2$
a_o	0.0414	1/K
T_o	373	K
T_m	260	°C
T_r	94.5	°C
n	0.2903	

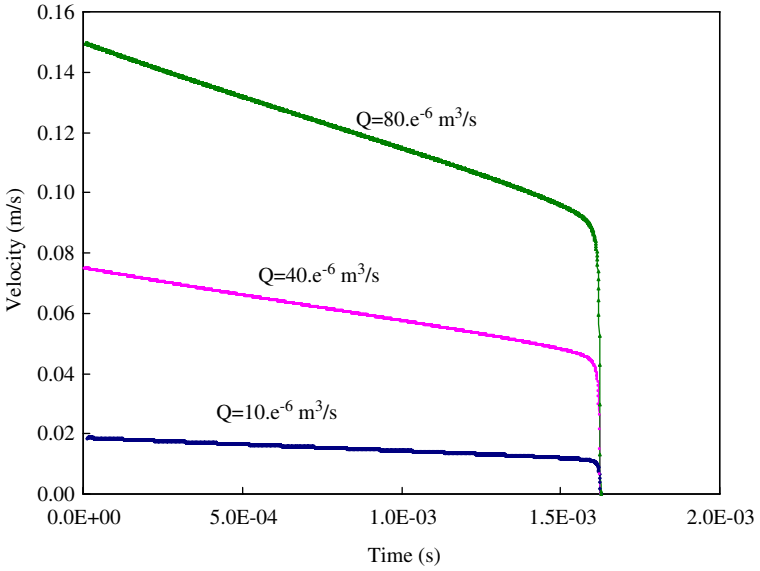

Fig. 4. Variations of velocity in the microchannel for different injection rates; $a = 100$ μm; $T_w = 90$ °C; $h_t = 10{,}000$ W/(m^2 °C).

the velocity decreases sharply to zero. Notice that the velocity depends on the viscosity related to the value of n for a power law flow. For different injection rates, the velocity drops to zero at the same time.

The radius of the microchannel is expected to have a large effect on the melt filling distance because of the influence of the heat transfer distance. Fig. 5 shows the polymer melt filling distance for different sizes of

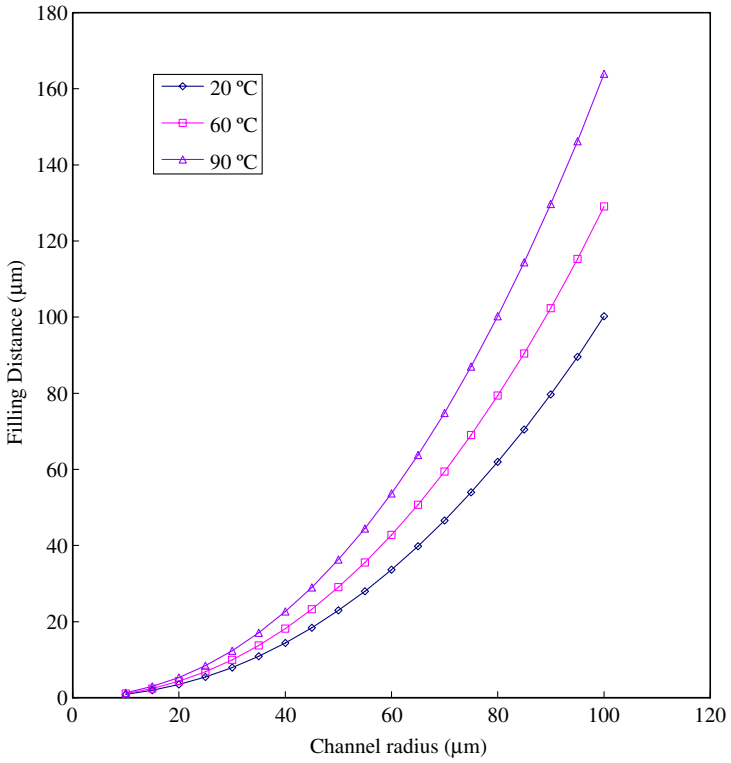

Fig. 5. Filling distance in the microchannels of different radius and mold temperatures; $Q = 80\,e^{-6}$ m^3/s; $h_t = 10{,}000$ W/(m^2 °C).

microchannels and mold temperatures. The filling rate in this case is 80×10^{-6} m^3/s. The filling distance increases dramatically with respect to the increase of the channel size. From Eq. (5), increase of the channel radius will increase the filling velocity because of the decrease of β. In additions, the microchannel with a large radius reduces the cooling speed of the polymer melt. Those effects lead to the large increase of filling distance for large channel. If the filling distance is divided by the corresponding channel radius, one can plot the maximum aspect ratio of a cylindrical channel that can be filled without short shot as shown in Fig. 6. If the mold

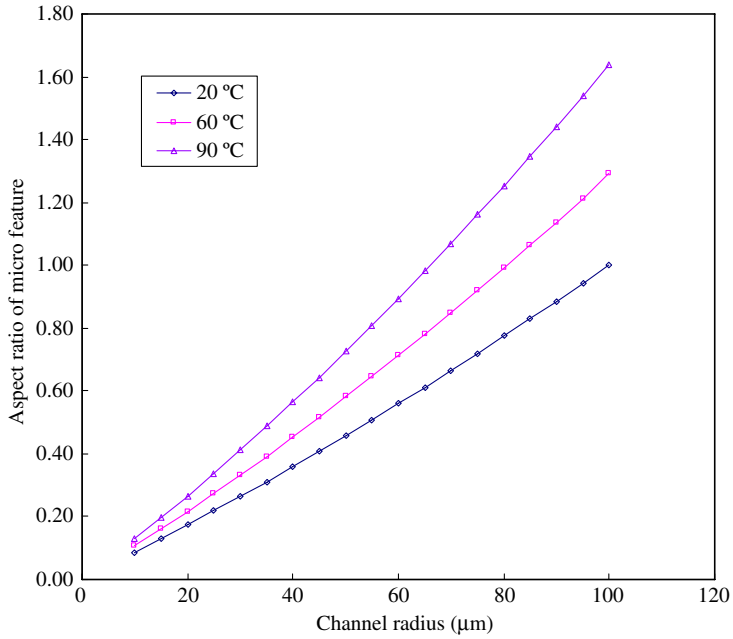

Fig. 6. Maximum aspect ratio of cylindrical channel that can be filled for different channel radius; $Q = 80\,e^{-6}$ m^3/s; $h_t = 10{,}000$ W/(m^2 °C).

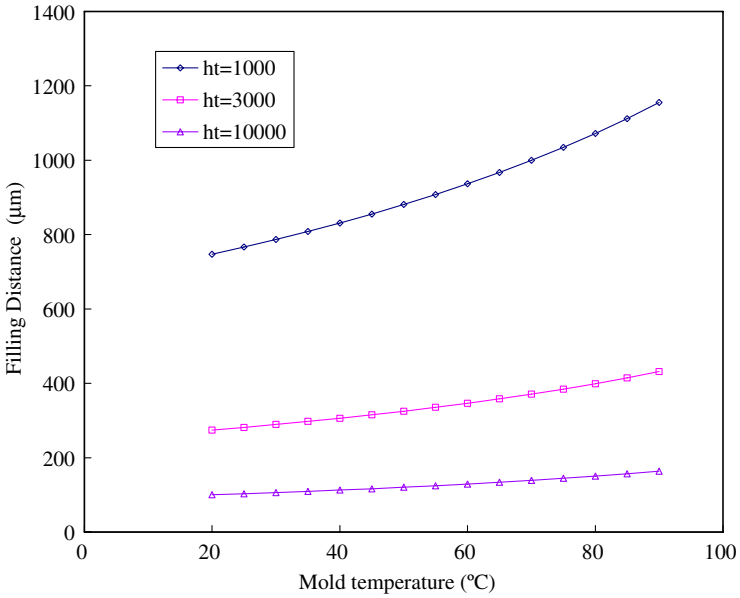

Fig. 7. Filling distance in the microchannel for different heat transfer coefficients and mold temperatures; $Q = 80\,e^{-6}$ m^3/s; $a = 100$ μm.

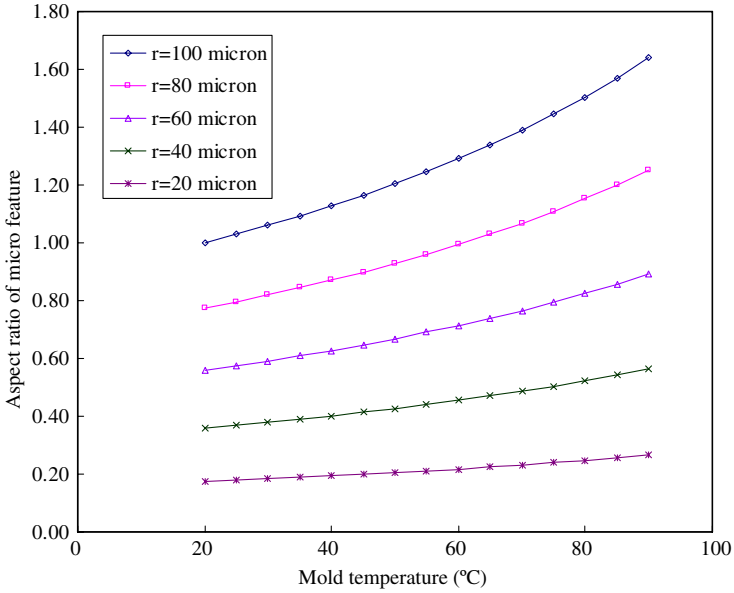

Fig. 8. Maximum aspect ratio of cylindrical channel that can be filled with respect to different mold temperatures; $Q = 80\,e^{-6}\,m^3/s$; $h_t = 10{,}000\ W/(m^2\,°C)$.

temperature is set to 20 °C, the cylindrical channel that can be filled completely must has an aspect ratio less than 1 for channel radius less than 100 μm. For molding with 90 °C mold temperature, a cylindrical channel with an aspect ratio higher than 1 can be completely filled for channel radius larger than 70 μm.

If the channel radius is set to 100 μm, the effect of mold temperature on the filling distance is shown in Fig. 7 for different values of heat transfer coefficients. As demonstrated previously, higher mold temperature will enhance the filling process and results in longer filling distance. The effect of the heat transfer coefficient on

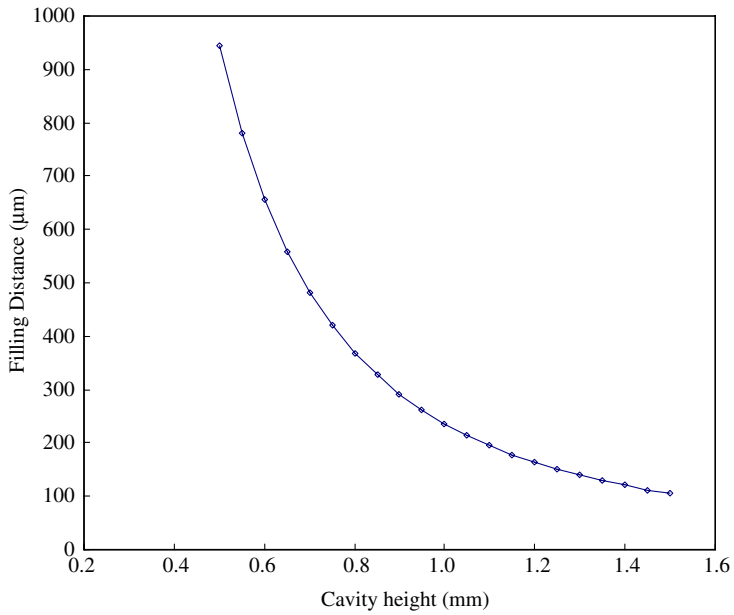

Fig. 9. Filling distance in the microchannel for different cavity heights; $a = 100\ \mu m$; $Q = 80 \times 10^{-6}\ m^3/s$; $T_w = 90\ °C$; $h_t = 10{,}000\ W/(m^2\,°C)$.

the filling distance is found to be profound as shown in the figure. For a lower value of heat transfer coefficient, $h_t = 1000$ W/(m^2 °C), the cooling rate from the mold wall is quite slow, resulting in a larger filling distance. As the heat transfer coefficient is higher, the cooling process is fast and the filling distance becomes very short. At the same time, the effect of mold temperature on the filling distance becomes less with a lower value of h_t. As the heat transfer coefficient is fixed, the aspect ratio of a microfeature that can be filled is plotted against the mold temperature in Fig. 8 for different sizes of cylindrical microchannels. The effect of mold temperature on the possible filled aspect ratio is less than that of channel radius as shown in Fig. 6.

In the current model, the filling of the microchannel depends on the pressure built up, P_o, at the entrance of the channel. As the melt front passes by the microchannel, the value of P_o is affected by the channel height, h. The effect of the channel height on the filling distance is shown in Fig. 9. The filling distance increases dramatically as the channel height decreases to 0.5 mm. It is concluded that in molding of components with microfeatures as those analyzed in this study, decrease of the part thickness could also enhance the filling in the microfeatures.

4. Conclusions

A simplified analytical model was constructed to estimate the injection distance into the microchannels of a molding component based on several ideal assumptions. In this analysis, the ability to fill the cylindrical microfeatures in a macrocomponent can be estimated. Effects of the processing and geometric parameters were explored using the model. The filling distance is found to strongly depend on the value of the heat transfer coefficient because of the strong dependence of the process on the thermal behavior. Although the heat transfer model is simplified to the steady two-dimensional analysis, the results still provide some insights for the relationship between the studied parameters and the microfilling distance, which will shed some light on the design of the process. The solution method could also extend to model other microgeometry following the same procedures. Only different governing equations for the flow and temperature must be solved for the corresponding geometry.

Acknowledgements

The authors would like to thank for the financial support from National Science Council in Republic of China under the Contract Number of NSC 91-2212-E006-131.

References

[1] E.C. Becker, W. Ehrfeld, P. Hagmann, A. Maner, D. Munchmeyer, Fabrication of microstructures with extreme structural heights by synchrotron radiation lithography, galvanoforming and plastic forming (LIGA process), Microelectron. Eng. 4 (1986) 35–56.
[2] Y. Cheng, B.Y. Shew, C.Y. Lin, D.H. Wei, M.K. Chyu, Ultra-deep LIGA process, J. Micromech. Microeng. 9 (1999) 58–63.
[3] M.J. Madou, L. Yu, G.C. Koh, L.J. Lee, K.W. Koelling, Experimental investigation and numerical simulation of injection molding with micro-features, Polym. Eng. Sci. 42 (5) (2002).
[4] L.J. Lee, M.J. Madou, S. Daunert, S. Lai, C.H. Shih, Design and fabrication of CD-like microfluidic platforms for diagnostic: microfluidic functions, Biomed. Microdevices 3 (4) (2001) 245–254.
[5] M.S. Despa, K.W. Kelly, J.R. Collier, Injection molding of polymeric LIGA HARMs, Microsyst. Technol. 6 (1999) 60–66.
[6] V. Piotter, K. Mueller, K. Plewa, R. Ruprecht, J. Hausselt, Performance and simulation of thermoplastic microinjection molding, Microsyst. Technol. 8 (2002) 387–390.
[7] B. Xu, K.T. Ooi, T.N. Wong, C.Y. Liu, Study on the viscosity of the liquid flowing in microgeometry, J. Micromech. Microeng. 9 (1999) 337–384.
[8] E.E. Rosenbaun, S.G. Hatzikiriakos, Wall slip in the capillary flow of molten polymers subject to viscous heating, AIChE J. 43 (1997) 598–608.
[9] V.S. Arpaci, Conduction Heat Transfer, Addison–Wesley, New York, 1980.